ChemPubSoc Europe

DOI: 10.1002/chem.201402697

CHEMISTRY
A European Journal
Communication

Janus Particles

Self-Assembly of Fullerene-Based Janus Particles in Solution: Effects of Molecular Architecture and Solvent

Zhiwei Lin,[a] Pengtao Lu,[a] Chih-Hao Hsu,[a] Kan Yue,[a] Xue-Hui Dong,[a] Hao Liu,[a] Kai Guo,[a] Chrys Wesdemiotis,[a, b] Wen-Bin Zhang,*[a, c] Xinfei Yu,*[a] and Stephen Z. D. Cheng*[a]

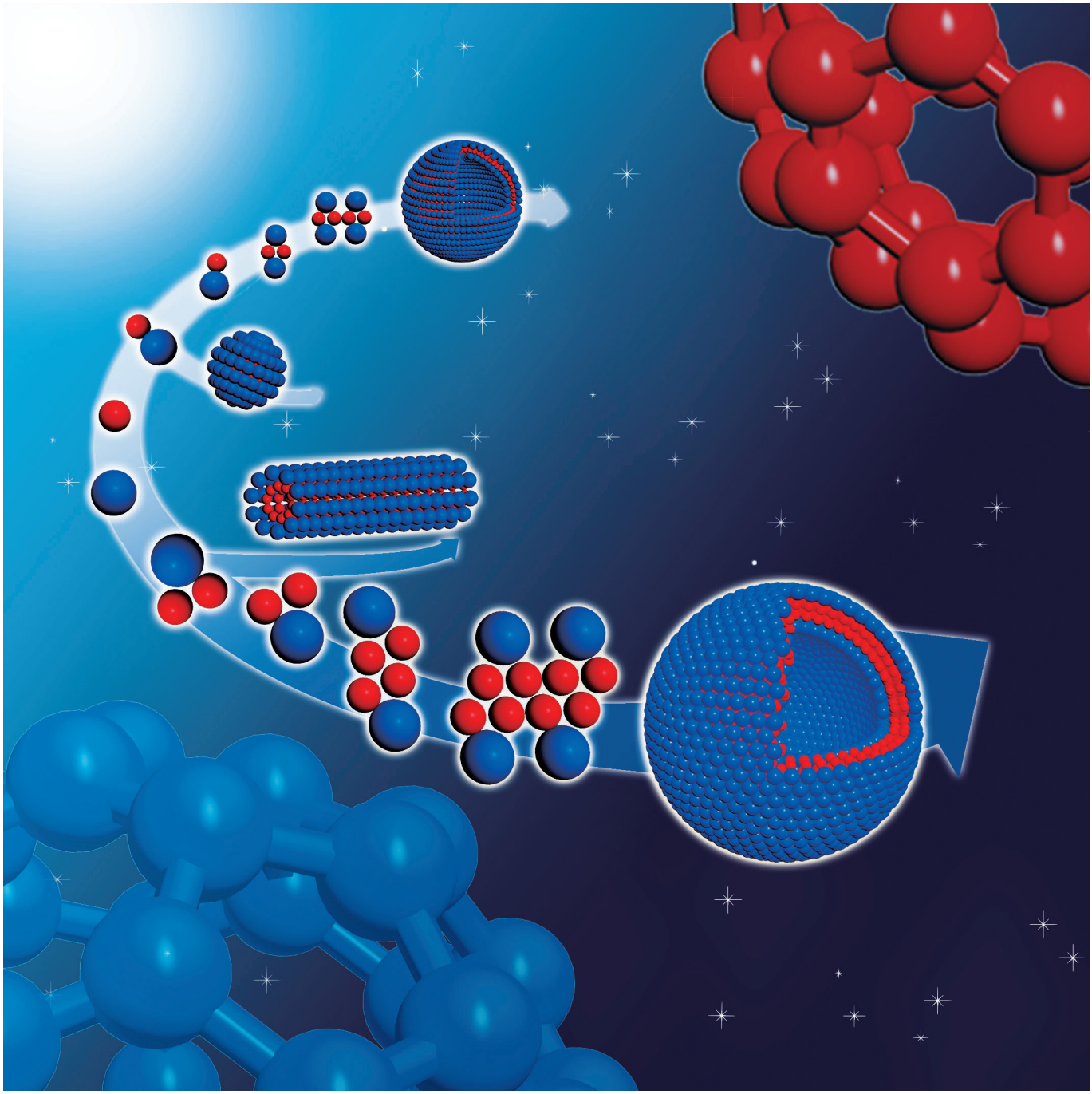

© 2014 Wiley-VCH Verlag GmbH & Co. KGaA, Weinheim

Abstract: Two molecular Janus particles based on amphiphilic [60]fullerene (C_{60}) derivatives were designed and synthesized by using the regioselective Bingel–Hirsh reaction and the click reaction. These particles contain carboxylic acid functional groups, a hydrophilic fullerene (AC_{60}), and a hydrophobic C_{60} in different ratios and have distinct molecular architectures: 1:1 (AC_{60}–C_{60}) and 1:2 (AC_{60}–$2C_{60}$). These molecular Janus particles can self-assemble in solution to form aggregates with various types of micellar morphology. Whereas vesicular morphology was observed for both AC_{60}–C_{60} and AC_{60}–$2C_{60}$ in tetrahydrofuran, in a mixture of *N*,*N*-dimethylformamide (DMF)/water, spherical micelles and cylindrical micelles were observed for AC_{60}–C_{60} and AC_{60}–$2C_{60}$, respectively. A mechanism of formation was tentatively proposed based on the effects of molecular architecture and solvent polarity on self-assembly.

Since the concept of "Janus grains" was introduced by de Gennes and co-workers,[1] tremendous attention has been paid on their symmetry-breaking structures, self-assembly behavior, and unique properties.[2] Progress have been made on the design and synthesis of organic/inorganic micellar or colloidal Janus particles with the availability of sophisticated synthetic techniques.[3] In those studies, the size of these Janus particles usually ranges from hundreds of nanometers to micrometers. If a Janus grain is based on a well-defined molecular structure with nanometer size and persistent shape, it may be considered a molecular Janus particle (MJP).[2c,4] There are two types of symmetry breaking for MJPs: geometric and chemical symmetry. Various efforts have so far been made to prepare MJPs with flexible conformations, example being amphiphilic dendrimers,[5] block copolymers,[6] and polymeric brushes,[7] all of which can self-assemble into intriguing structures in bulk[5a] and solution.[5b,c] However, the construction of MJPs as precisely-defined molecular nanoparticles of fixed shape, volume, and functionality that can retain their asymmetrical geometry and chemistry during self-assembly remains largely unexplored.

Recently, molecular nanoparticles have been conceptually proposed as the elemental nano-building blocks, or "nano-atoms" for building precise macromolecules.[4] Nano-atoms are shape- and volume-persistent molecular nanoparticles, such as [60]fullerene (C_{60}), polyhedral oligomeric silsesquioxanes (POSS), polyoxometalates (POM), and folded globular proteins.[4] They possess precisely-defined primary chemical structures and surface functionalities, and are ready for precise synthesis of giant molecules utilizing efficient methods such as the sequential click approach.[8] MJPs based on POSS[9] and POM[10] derivatives have been reported to self-organize into bilayer structures in the bulk. Yet the examples are rare. It is thus of interest to further expand the scope of MJPs and investigate how they can be directed to assemble into different hierarchical structures, and how to further promote transformations and amplifications of microscopic functionalities towards macroscopic properties.[9a,11]

Among those molecular nanoparticles, C_{60} is a spherical nanoparticle with truncated icosahedral (I_h) symmetry. Surfaces of C_{60} can be precisely functionalized by regioselective chemical reactions.[12] Several C_{60}-based amphiphiles have exhibited interesting self-assembly behaviors in solution.[13] For instance, a series of pentasubstituted fullerene potassium salts can self-assemble into bilayer vesicles in THF/water.[13d–f] We have recently synthesized new C_{60} derivatives bearing ten carboxylic acid functional group (AC_{60}) and further tethered them with one or two polystyrene (PS) tails to construct a new class of giant surfactants.[14] With increasing initial molecular concentration or the PS tail length, micellar morphologies can be tuned from spheres, to cylinders, and finally, to vesicles. The PS tails are recognized to be stretched in their micelles, similar to small molecular surfactants.[8c,14–15]

Herein, we report on the design, synthesis, and self-assembly of two new MJPs based on C_{60}, namely, AC_{60}–C_{60} and AC_{60}–$2C_{60}$, by clicking a hydrophilic AC_{60} with one or two hydrophobic C_{60}. The resulting amphiphilic MJPs are expected to exhibit self-assembly behaviors that depend on the solvent system.

AC_{60}–C_{60} and AC_{60}–$2C_{60}$ are synthesized by combining the regioselective Bingel–Hirsh reaction[16] and the highly efficient Huisgen 1,3-dipolar cycloaddition click reaction,[17] as outlined in Scheme 1. Monotethered C_{60} derivative **2** with an azide group was prepared by reaction of compound **1** with C_{60} under the Bingel reaction conditions.[16a] Precisely defined [5:1]-hexakisadducts of C_{60}, with one (**3a**) or two (**3b**) terminal alkyne groups and ten protected carboxylic acid groups, were synthesized based on the procedures described in our previous publication.[14] The azide–alkyne click reaction[18] was successfully utilized to link the monofunctionalized C_{60} (**2**) with the surface-modified C_{60} derivatives (**3a**–**b**) in high yields ($\geq$ 80%), resulting in conjugates of a protected carboxylic acid group functionalized C_{60} tethered with one (**4a**, tC_{60}–C_{60}) or two C_{60}s (**4b**, tC_{60}–$2C_{60}$). The disappearance of the azide resonance at ca. 2100 cm^{-1} and the alkyne resonance at ca. 3300 cm^{-1} in the IR spectra of **4a**–**b** provides evidence of the successful reaction between **2** and **3a**–**b** (see Figure S1 in

[a] *Z. Lin, P. Lu, C.-H. Hsu, Dr. K. Yue, Dr. X.-H. Dong, H. Liu, K. Guo, Prof. C. Wesdemiotis, Dr. W.-B. Zhang, Dr. X. Yu, Prof. S. Z. D. Cheng*
Department of Polymer Science
College of Polymer Science and Polymer Engineering
The University of Akron, 170 University Ave.
Akron, Ohio, 44325-3909 (USA)
Fax: (+1) 330-972-8626
E-mail: wenbin@pku.edu.cn
xy5@zips.uakron.edu
scheng@uakron.edu

[b] *Prof. C. Wesdemiotis*
Department of Chemistry
The University of Akron
Akron, Ohio, 44325-3601 (USA)

[c] *Dr. W.-B. Zhang*
Key Laboratory of Polymer Chemistry & Physics of Ministry of Education
College of Chemistry and Molecular Engineering
Center for Soft Matter Science and Engineering
Peking University, Beijing 100871 (P. R. China)

Supporting information for this article is available on the WWW under http://dx.doi.org/10.1002/chem.201402697.

© 2014 Wiley-VCH Verlag GmbH & Co. KGaA, Weinheim

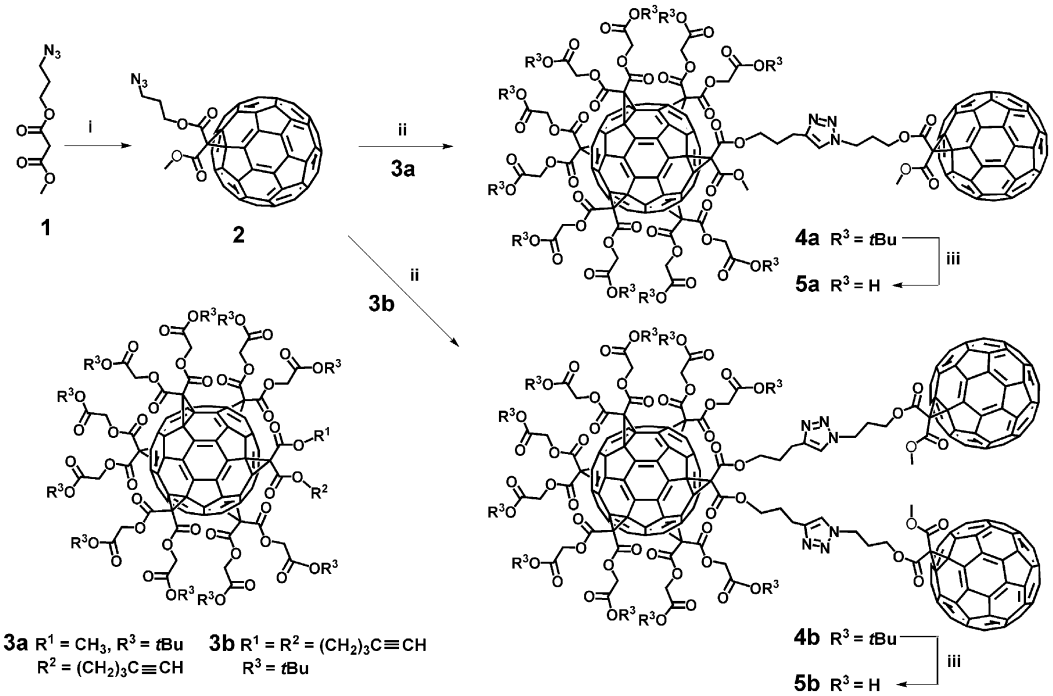

Scheme 1. Synthetic route to AC_{60}–C_{60} and AC_{60}–2C60. Reaction conditions: i) C60, toluene, I_2, DBU, RT (**2**, 51%); ii) toluene, CuBr, PMDETA, RT (**4a**, 81%; **4b**, 80%); iii) CH_2Cl_2, CF_3COOH, RT (**5a**, >90%; **5b**, >90%). DBU = 1,8-diazabicyclo[5.4.0]undec-7-ene, PMDETA = *N*,*N*,*N*′,*N*″,*N*″-pentamethyldiethylenetriamine.

the Supporting Information). The amphiphilic final products, namely, AC_{60}–C_{60} (**5a**) and AC_{60}–$2C_{60}$ (**5b**), were obtained upon deprotection of the *tert*-butyl esters groups of **4a**–**b**. Chemical structures of AC_{60}–C_{60} and AC_{60}–$2C_{60}$ were unambiguously confirmed by their ^{1}H NMR and ^{13}C NMR spectra (see Figures S2–S5 in the Supporting Information). Moreover, the most convincing evidence is given by matrix-assisted laser desorption/ionization time-of-flight (MALDI-TOF) mass spectra as shown in Figure 1. Monoisotopic mass peaks observed at m/z = 2911.3 for AC_{60}–C_{60} and 3882.4 for AC_{60}–$2C_{60}$ are in good agreement

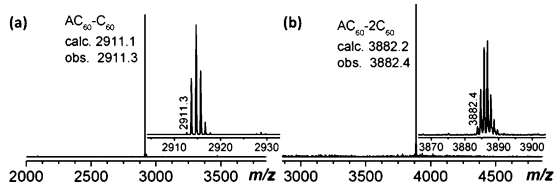

Figure 1. MALDI-TOF mass spectra of a) AC_{60}–C_{60} and b) AC_{60}–$2C_{60}$.

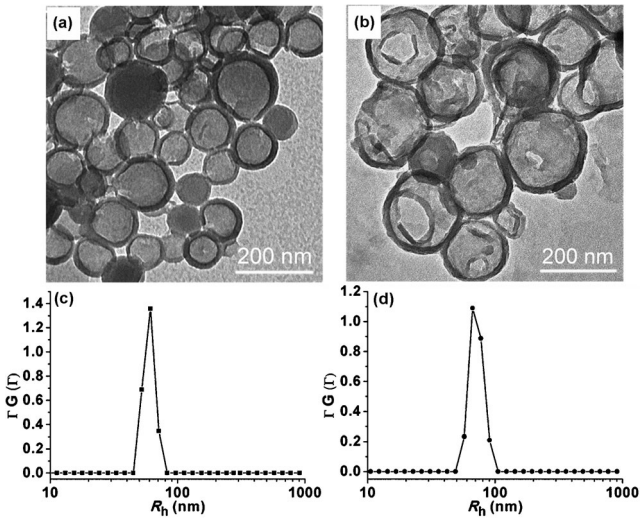

Figure 2. TEM images and DLS results of self-assembled vesicles of a) and c) for AC_{60}–C_{60}, b) and d) for AC_{60}–$2C_{60}$ in THF.

with the calculated values, which are 2911.1 and 3882.2, respectively.

The micellar behaviors of these MJPs are of great interest because they possess distinct molecular architectures and consist of shape and volume-persistent molecular nanoparticles. Self-assembly of these MJPs in solution was investigated by using two different strategies (see the Supporting Information for details). For both AC_{60}–C_{60} and AC_{60}–$2C_{60}$, when following the first strategy, vesicles were observed in THF, as suggested by the bright-field TEM images shown in Figure 2a and 2b. The overall layer thicknesses of these vesicles was measured to be around 12–16 nm from TEM images. Because the layer thickness values are much larger than the long-axis dimensions of AC_{60}–C_{60} and AC_{60}–$2C_{60}$, which are ca. 4 nm in the fully extended conformation (see Figure S6 in the Supporting Information), it is suggested that the vesicles are constructed by a double-layer molecular packing model.[13d–f,19] The vesicular morphologies were further confirmed by light scattering ex-

© 2014 Wiley-VCH Verlag GmbH & Co. KGaA, Weinheim

periments. As shown in Figure 2c and 2d, the hydrodynamic radii (R_h) of the vesicles obtained from dynamic light scattering (DLS) measurements are ca. 60 nm and ca. 79 nm for AC_{60}–C_{60} and AC_{60}–$2C_{60}$, respectively, values that are consistent with the average radii measured from TEM images (ca. 57 nm for AC_{60}–C_{60} and ca. 82 nm for AC_{60}–$2C_{60}$). Furthermore, the radii of gyration (R_g) of the vesicles measured by static light scattering (SLS) are ca. 56 and ca. 79 nm, respectively (see Figure S7 in the Supporting Information). The measured ratios of R_g/R_h are thus both close to unity (0.93 for AC_{60}–C_{60} and 1.0 for AC_{60}-$2C_{60}$), validating the formation of self-assembled vesicular structures.[13f]

The driving force for micellar formation in THF must be attributed to the aggregation of hydrophobic C_{60} particles because THF is a poor solvent for C_{60} at room temperature. Therefore, the outer and inner layers of the vesicles are formed by AC_{60}, while the hydrophobic C_{60}s are located in the middle region between these two AC_{60} layers to form a bilayer structure in the vesicles. This is also consistent with the previously reported self-assembled bilayer vesicles from amphiphilic fullerene derivatives in fullerene-phobic solvents.[13d–f,19] Interestingly, when the vesicles are subjected to ultrasonication in THF solution, the measured R_h value remains constant for at least 5 h (see Figure S8 in the Supporting Information), indicating that the vesicles prepared in THF are quite stable and robust. This can be attributed to the π–π interaction between the hydrophobic C_{60}s (minor) and the strong hydrogen-bonding interaction between the hydrophilic AC_{60}s (major).

To reveal the effect of molecular architectures on the self-assembly behaviors of these two MJPs, we further studied their self-assembly in DMF/water following the second strategy. The critical water concentrations (C_{CWC}) for AC_{60}–C_{60} and AC_{60}–$2C_{60}$ to form micelles were determined to be 13.7 wt% and 2.2 wt%, respectively (see Figure S9 in the Supporting Information). The difference in the C_{CWC} values can be attributed to the largely increased hydrophobicity of AC_{60}–$2C_{60}$ compared to AC_{60}–C_{60}. Despite the C_{CWC} difference, we choose to explore and compare the morphologies of these two self-assembled MJPs at relatively high and identical water contents. Therefore, AC_{60}–C_{60} and AC_{60}–$2C_{60}$ were first dissolved in DMF at an initial concentration of 0.5 wt% and then water was added dropwise to reach a final water content of 80 wt%. Surprisingly, spherical micelles with an average diameter of ca. 8 nm are observed for AC_{60}–C_{60}, as shown in Figure 3a; while worm-like cylinders with an average diameter of ca. 13 nm and an aspect ratio larger than 10 are observed for AC_{60}–$2C_{60}$ under identical conditions (Figure 3b).

To obtain the average macroscopic values of these micelles, DLS experiments were performed. As shown in Figure S10 in the Supporting Information, the R_h of the spherical micelles from AC_{60}–C_{60} has a relatively broad distribution centered at around 3 nm, which is qualitatively consistent with that measured from TEM images. The formation of cylinders from AC_{60}–$2C_{60}$ can also be verified by the fact that the R_h values vary upon changing the scattering angles in DLS experiments (see Figure S11 in the Supporting Information). The R_h value of the cylinders is estimated to be 115 ± 10 nm by extrapolating the scattering angles to zero, as shown in Figure S12 in the Supporting Information. Furthermore, the R_g values of the cylinders was measured to be ca. 308 ± 5 nm (see Figure S13 in the Supporting Information). The ratio of R_g/R_h is thus ca. 2.7, which further confirms the formation of cylinders from AC_{60}–$2C_{60}$.

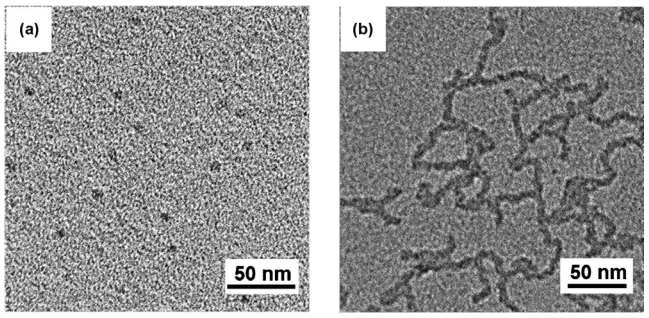

Figure 3. TEM images of the self-assembled micelles of a) AC_{60}–C_{60} and b) AC_{60}–$2C_{60}$ in the solution of DMF with an initial concentration of 0.5 wt%; water was added dropwise to reach a water content of 80 wt%.

The formation of micelles with various morphologies from these two MJPs could be rationalized as put forward by Israelachvili et al.[20] The self-assembled structures of amphiphiles can be predicted by the packing parameter (P), which is defined as:

$$P = V/(Al_c)$$

where V is the volume occupied by the hydrophobic moiety, l_c is the critical length of the hydrophobic moiety, and A is the optimal area occupied by the hydrophilic moiety.

Based on this argument, the preferred self-assembled structures of amphiphilic molecules vary with increasing P from spheres ($P < 1/3$), to cylinders ($1/3 < P < 1/2$), to vesicles ($1/2 < P < 1$). In our system, because hydrophobic C_{60} possesses a well-defined structure with a fixed volume, the value of V_{C60} and l_{C60} can be obtained from the volume and diameter of C_{60}, respectively ($V_{C60} = 0.52$ nm^3 and $l_{C60} = 1$ nm).[21] For the hydrophilic AC_{60}, its smallest A_{AC60} can be estimated to be 1.5 nm^2 in the solution without considering solvation of the surface carboxylic acid groups.[22] This serves as the lowest limit for the value of A_{AC60}. When using these values to calculate the P value of AC_{60}–C_{60} and AC_{60}–$2C_{60}$, it turns out that $P_{AC60-C60} = 0.35$ ($\geq 1/3$) and $P_{AC60-2C60} = 0.69$ ($> 1/2$), indicating that the micelles of AC_{60}–C_{60} are near the boundaries between the cylinders and spheres (but on the cylinder side), while the micelles of AC_{60}–$2C_{60}$ are located in the vesicular phase.

In reality, however, the hydrodynamic size of AC_{60} is expected to increase as the degree of ionization (α) of carboxylic acid groups increases.[14] Therefore, it is necessary to consider the effect of the value of α on the value of A_{AC60} in pure THF and the mixture of DMF/water. The α value can be estimated based on the results of FT-IR spectroscopy as a first approximation.[15] Figures S14 and S15 in the Supporting Information show four FT-IR spectra of the micelle solutions prepared in

© 2014 Wiley-VCH Verlag GmbH & Co. KGaA, Weinheim

both THF and DMF/water mixtures for two samples. The highlighted absorption bands at ca. 1740 cm^{-1} and ca. 1620 cm^{-1} are attributed to the C=O stretching band of the native COOH and ionized group COO^-, respectively.[15] As exhibited in Figure S14a and S15a in the Supporting Information, because the α value of carboxylic acid groups for AC_{60} in THF is rather low (ca. 20%), the A value of AC_{60} in THF can still be approximated by 1.5 nm^2. It gives rise to a P value of 0.35 and 0.69 for AC_{60}–C_{60} and AC_{60}–$2C_{60}$ in THF, respectively. Based on this estimation, we should observe micelles of cylindrical morphology ($1/3 < P < 1/2$) for AC_{60}–C_{60} and of vesicular morphology ($1/2 < P < 1$) for AC_{60}–$2C_{60}$. In Figure 2, the vesicles are indeed observed for AC_{60}–$2C_{60}$. However, experimentally, AC_{60}–C_{60} also forms vesicles in THF, which differs from that predicted by using calculations.

To provide a reasonable explanation for this discrepancy, we put our argument forward in the following way: as described above, AC_{60} particles are located at both the outside and the inside surfaces of the vesicles, while the C_{60} particles are located in the middle of the vesicles owing to the poor solubility of C_{60} in THF. We further propose that within the vesicles of AC_{60}–C_{60}, the C_{60} particles are arranged in an interdigitated packing manner (Figure 4a). In contrast, the C_{60} particles form a bilayer within the vesicles of AC_{60}–$2C_{60}$, as schematically shown in Figure 4b. This is similar to reported fullerene amphiphiles.[13e] In this argument, the geometrical arrangement for both cases becomes identical with the same cross-section areas, but differences in molecular packing topologies.

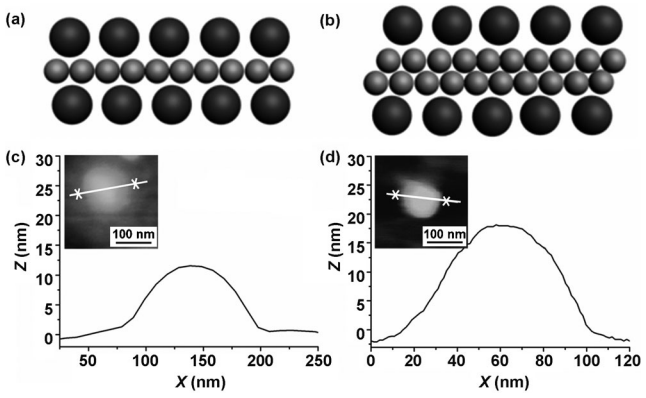

Figure 4. Schematic illustrations of two packing models of vesicles. a) Interdigitated structure for AC_{60}–C_{60} and b) bilayer structure for AC_{60}–$2C_{60}$. AFM height profiles of vesicles formed by c) AC_{60}–C_{60} and d) AC_{60}–$2C_{60}$ in THF. Insets are AFM images of two individual vesicles.

To verify the proposed packing models, atomic force microscopy (AFM) was used to measure the layer thickness of the collapsed vesicles after evaporating the solvent. Only those vesicles possessing smooth surface were selected to measure their heights, as illustrated by the two typical height profiles shown in Figures 4c and 4d. The average thickness of vesicles obtained from ten independent measurements are 12.5 ± 1.3 nm for AC_{60}–C_{60}, and 16.2 ± 1.5 nm for AC_{60}–$2C_{60}$, resulting in a ratio of 0.77 between the two thickness values. The theoretical double-thickness values of interdigitated layers and bilayers are calculated as 7.6 nm and 9.6 nm, respectively, by assuming that the diameter of C_{60} is 1.0 nm and that the diameter of AC_{60} is 1.4 nm (which is estimated from $A_{AC60} = 1.5$ nm^2 in THF). Because it is difficult for the layers of C_{60} and AC_{60} to pack closely after micelle collapse, the theoretical thicknesses of interdigitated layers and bilayers are smaller than the measured ones. Nevertheless, the theoretically calculated ratio between the thickness values of interdigitated layers and bilayers is 0.79, which is in good agreement with the measured ratio (0.77). Therefore, the bilayer and interdigitated packing models are at least partially confirmed.

In the DMF/water system, a much higher α value is observed (ca. 50%), which results in a larger A value of AC_{60}. As a result, as long as $A > 1.5$ nm^2, $P_{AC60-C60}$ would decrease to below 1/3, suggesting a sphere morphology. In the case of AC_{60}–$2C_{60}$, it is even more difficult to estimate the $P_{AC60-2C60}$ value. We speculate that it is between 1/3 and 1/2, when the A_{AC60} value is in somewhere between 2.1 and 3.1 nm^2, suggesting micelles of cylindrical morphology in the mixture of DMF/water.

In summary, two precisely defined fullerene-based MJPs with distinct molecular architectures (AC_{60}–C_{60} and AC_{60}–$2C_{60}$) were designed and synthesized through regioselective sequential Bingel–Hirsh reactions and click reactions. Self-assembly of these two MJPs has been investigated in solution. In THF, vesicles with interdigitated and bilayer molecular packing arrangements have been observed for AC_{60}–C_{60} and AC_{60}–$2C_{60}$, respectively. In the DMF/water system, however, micelles of spherical and cylindrical morphology are formed for AC_{60}–C_{60} and AC_{60}–$2C_{60}$, respectively. The degree of ionization of the carboxylic acid groups on AC_{60} plays an essential role in influencing their packing parameters (P) and determining the micelle morphology in different solvent systems. This work introduces a new approach to the design of molecular Janus grains, their precision synthesis, and diverse self-assembly behaviors in solution. It may expand the scope of traditional amphiphilic molecules and provide a platform to further study the self-assembly behaviors of shape-persistent MJPs.

Acknowledgements

This work was supported by National Science Foundation (DMR-0906898 and 1408872) and the Joint-Hope Education Foundation. The authors acknowledge Dr. Panchao Yin and Prof. Tianbo Liu for the help with light scattering experiments and analyses; Yan Sun and Prof. Alamgir Karim for the assistance in AFM experiments; and Jie Yu and Prof. Steven Chuang for offering kind help in FT-IR tests and analyses. Dr. Chrys Wesdemiotis and Kai Guo also thank the financial support from NSF (CHE-1012636).

Keywords: fullerenes · Janus particles · micelles · self-assembly · vesicles

[1] P. G. de Gennes, *Angew. Chem.* **1992**, *104*, 856–859; *Angew. Chem. Int. Ed. Engl.* **1992**, *31*, 842–845.

© 2014 Wiley-VCH Verlag GmbH & Co. KGaA, Weinheim

[2] a) S. Granick, S. Jiang, Q. Chen, *Phys. Today* **2009**, *62*, 68 – 69; b) A. Walther, A. H. E. Müller, *Soft Matter* **2008**, *4*, 663 – 668; c) M. Lattuada, T. A. Hatton, *Nano Today* **2011**, *6*, 286 – 308.

[3] a) D. Dendukuri, D. C. Pregibon, J. Collins, T. A. Hatton, P. S. Doyle, *Nat. Mater.* **2006**, *5*, 365 – 369; b) Z. Nie, W. Li, M. Seo, S. Xu, E. Kumacheva, *J. Am. Chem. Soc.* **2006**, *128*, 9408 – 9412; c) H. Yu, M. Chen, P. M. Rice, S. X. Wang, R. L. White, S. Sun, *Nano Lett.* **2005**, *5*, 379 – 382.

[4] W.-B. Zhang, X. Yu, C.-L. Wang, H.-J. Sun, I.-F. Hsieh, Y. Li, X.-H. Dong, K. Yue, R. Van Horn, S. Z. D. Cheng, *Macromolecules* **2014**, *47*, 1221 – 1239.

[5] a) V. Percec, M. R. Imam, T. K. Bera, V. S. K. Balagurusamy, M. Peterca, P. A. Heiney, *Angew. Chem.* **2005**, *117*, 4817 – 4823; *Angew. Chem. Int. Ed.* **2005**, *44*, 4739 – 4745; b) V. Percec, *Science* **2010**, *328*, 1009 – 1014; c) M. Yang, W. Wang, F. Yuan, X. Zhang, J. Li, F. Liang, B. He, B. Minch, G. Wegner, *J. Am. Chem. Soc.* **2005**, *127*, 15107 – 15111.

[6] a) L. Cheng, G. Hou, J. Miao, D. Chen, M. Jiang, L. Zhu, *Macromolecules* **2008**, *41*, 8159 – 8166; b) L. Cheng, G. Zhang, L. Zhu, D. Chen, M. Jiang, *Angew. Chem.* **2008**, *120*, 10325 – 10328; *Angew. Chem. Int. Ed.* **2008**, *47*, 10171 – 10174.

[7] M. Zhang, A. H. E. Müller, *J. Polym. Sci. Part A* **2005**, *43*, 3461 – 3481.

[8] a) X. Yu, K. Yue, I.-F. Hsieh, Y. Li, X.-H. Dong, C. Liu, Y. Xin, H.-F. Wang, A.-C. Shi, G. R. Newkome, R.-M. Ho, E.-Q. Chen, W.-B. Zhang, S. Z. D. Cheng, *Proc. Natl. Acad. Sci. USA* **2013**, *110*, 10078 – 10083; b) K. Yue, C. Liu, K. Guo, X. Yu, M. Huang, Y. Li, C. Wesdemiotis, S. Z. D. Cheng, W.-B. Zhang, *Macromolecules* **2012**, *45*, 8126 – 8134; c) Z. Wang, Y. Li, X.-H. Dong, X. Yu, K. Guo, H. Su, K. Yue, C. Wesdemiotis, S. Z. D. Cheng, W.-B. Zhang, *Chem. Sci.* **2013**, *4*, 1345 – 1352.

[9] a) H.-J. Sun, Y. Tu, C.-L. Wang, R. M. Van Horn, C.-C. Tsai, M. J. Graham, B. Sun, B. Lotz, W.-B. Zhang, S. Z. D. Cheng, *J. Mater. Chem.* **2011**, *21*, 14240 – 14247; b) Y. Li, W.-B. Zhang, I.-F. Hsieh, G. Zhang, Y. Cao, X. Li, C. Wesdemiotis, B. Lotz, H. Xiong, S. Z. D. Cheng, *J. Am. Chem. Soc.* **2011**, *133*, 10712 – 10715.

[10] M.-B. Hu, Z.-Y. Hou, W.-Q. Hao, Y. Xiao, W. Yu, C. Ma, L.-J. Ren, P. Zheng, W. Wang, *Langmuir* **2013**, *29*, 5714 – 5722.

[11] S. C. Glotzer, M. J. Solomon, *Nat. Mater.* **2007**, *6*, 557 – 562.

[12] a) A. Hirsch, M. Brettreich, *Fullerenes: Chemistry and Reactions*, Wiley-VCH, Weinheim, **2005**; b) A. Hirsch, O. Vostrowsky, *Eur. J. Org. Chem.* **2001**, 829 – 848.

[13] a) M. Brettreich, S. Burghardt, C. Böttcher, T. Bayerl, S. Bayerl, A. Hirsch, *Angew. Chem.* **2000**, *112*, 1915 – 1918; *Angew. Chem. Int. Ed.* **2000**, *39*, 1845 – 1848; b) S. Burghardt, A. Hirsch, B. Schade, K. Ludwig, C. Böttcher, *Angew. Chem.* **2005**, *117*, 3036 – 3039; *Angew. Chem. Int. Ed.* **2005**, *44*, 2976 – 2979; c) D. M. Guldi, F. Zerbetto, V. Georgakilas, M. Prato, *Acc. Chem. Res.* **2005**, *38*, 38 – 43; d) T. Homma, K. Harano, H. Isobe, E. Nakamura, *Angew. Chem.* **2010**, *122*, 1709 – 1712; *Angew. Chem. Int. Ed.* **2010**, *49*, 1665 – 1668; e) T. Homma, K. Harano, H. Isobe, E. Nakamura, *J. Am. Chem. Soc.* **2011**, *133*, 6364 – 6370; f) S. Zhou, C. Burger, B. Chu, M. Sawamura, N. Nagahama, M. Toganoh, U. E. Hackler, H. Isobe, E. Nakamura, *Science* **2001**, *291*, 1944 – 1947.

[14] X. Yu, W.-B. Zhang, K. Yue, X. Li, H. Liu, Y. Xin, C.-L. Wang, C. Wesdemiotis, S. Z. D. Cheng, *J. Am. Chem. Soc.* **2012**, *134*, 7780 – 7787.

[15] X. Yu, S. Zhong, X. Li, Y. Tu, S. Yang, R. M. Van Horn, C. Ni, D. J. Pochan, R. P. Quirk, C. Wesdemiotis, W.-B. Zhang, S. Z. D. Cheng, *J. Am. Chem. Soc.* **2010**, *132*, 16741 – 16744.

[16] a) C. Bingel, *Chem. Ber.* **1993**, *126*, 1957 – 1959; b) A. Hirsch, I. Lamparth, T. Grösser, H. R. Karfunkel, *J. Am. Chem. Soc.* **1994**, *116*, 9385 – 9386; c) A. Hirsch, I. Lamparth, H. R. Karfunkel, *Angew. Chem.* **1994**, *106*, 453 – 455; *Angew. Chem. Int. Ed. Engl.* **1994**, *33*, 437 – 438.

[17] H. C. Kolb, M. G. Finn, K. B. Sharpless, *Angew. Chem.* **2001**, *113*, 2056 – 2075; *Angew. Chem. Int. Ed.* **2001**, *40*, 2004 – 2021.

[18] W.-B. Zhang, Y. Tu, R. Ranjan, R. M. Van Horn, S. Leng, J. Wang, M. J. Polce, C. Wesdemiotis, R. P. Quirk, G. R. Newkome, S. Z. D. Cheng, *Macromolecules* **2008**, *41*, 515 – 517.

[19] A. M. Cassell, C. L. Asplund, J. M. Tour, *Angew. Chem.* **1999**, *111*, 2565 – 2568; *Angew. Chem. Int. Ed.* **1999**, *38*, 2403 – 2405.

[20] J. N. Israelachvili, *Intermolecular and Surface Forces*, 3edrd edElsevier, **2011**, pp. 535 – 550.

[21] H. W. Kroto, J. R. Heath, S. C. O'Brien, R. F. Curl, R. E. Smalley, *Nature* **1985**, *318*, 162 – 163.

[22] I. Lamparth, C. Maichle-Mössmer, A. Hirsch, *Angew. Chem.* **1995**, *107*, 1755 – 1757; *Angew. Chem. Int. Ed. Engl.* **1995**, *34*, 1607 – 1609.

Received: March 20, 2014
Published online on July 22, 2014

© 2014 Wiley-VCH Verlag GmbH & Co. KGaA, Weinheim